Original Article

Quantification of bone quality and distribution of the proximal humerus with dual-energy computed tomography

Qinqin Yu[1]^, Jia Yang[1], Chenwei Zhou[1], Zhihan Xu[2], Chao Liu[1], Qian Luo[1], Lei Zhang[1]

[1]Department of Radiology, Shanghai General Hospital, Shanghai Jiao Tong University School of Medicine, Shanghai, China; [2]Siemens Healthineers, Shanghai, China

Contributions: (I) Conception and design: Q Yu, L Zhang; (II) Administrative support: L Zhang, Q Luo; (III) Provision of study materials or patients: Q Yu, J Yang, C Zhou, Z Xu, C Liu; (IV) Collection and assembly of data: Q Yu, J Yang, C Zhou, C Liu; (V) Data analysis and interpretation: Q Yu, J Yang, L Zhang; (VI) Manuscript writing: All authors; (VII) Final approval of manuscript: All authors.

Correspondence to: Lei Zhang, Doctor/Professor. Department of Radiology, Shanghai General Hospital, Shanghai Jiao Tong University School of Medicine, No. 650 New Songjiang Road, Songjiang District, Shanghai 201620, China. Email: lei.zhang2@shgh.cn.

Background: The proximal humerus is a common site of osteoporotic fractures, and bone quality is a predictor of surgical reduction quality. Dual-energy computed tomography (DECT) is assuming an increasingly important role in the quantification of bone mineral density (BMD) due it is ability to perform three-material decomposition. We aimed to analyze the bone quality and distribution of the proximal humerus with DECT quantitatively.

Methods: Sixty-five consecutive patients (average age 49.5±15.2 years; male: female ratio 32:33) without proximal humerus fractures who had undergone DECT were retrospectively selected. The humeral head was divided into 4 regions on a cross section in the medial plane between the greater tuberosity and the surgical neck. The quantitative parameters, including virtual noncalcium (VNCa) value, computed tomography value of calcium (CaCT), computed tomography value of mixed-energy images (regular CT value) (rCT), and relative calcium density (rCaD), were measured. The correlations between the quantitative parameters and age and body mass index (BMI) were analyzed, and the correlations of age, sex, BMI, region of the humeral head, and VNCa value on CaCT were evaluated.

Results: The differences in CaCT, rCT, and rCaD between the 4 regions of proximal humerus were statistically significant (P<0.001), while the difference in VNCa values was not (P=0.688). The calcium concentration (CaCT and rCaD) was the densest in the posteromedial zone. The differences of CaCT, rCT, and rCaD between males and females in the 4 regions of proximal humerus were statistically significant (P<0.05), while those of the posterolateral zone were not (rCT; P>0.05). The differences in VNCa values between males and females were also not significant (P>0.05). Multivariable linear regression analysis indicated that sex, age, BMI, regions, and VNCa were significant (P<0.05) predictors of the CaCT value.

Conclusions: The concentration of calcium was the densest in the posteromedial region of proximal humerus, and the VNCa value of DECT may be used for quantifying the BMD of the proximal humerus.

Keywords: Proximal humerus; dual-energy computed tomography (DECT); virtual noncalcium (VNCa); bone mineral density (BMD)

Submitted Sep 05, 2022. Accepted for publication Jul 07, 2023. Published online Jul 20, 2023.
doi: 10.21037/qims-22-927
View this article at: https://dx.doi.org/10.21037/qims-22-927

^ ORCID: 0000-0002-0256-4083.

Introduction

The proximal humerus is a common site of osteoporotic fractures. Various surgical treatment options have been described and are still being debated; regardless, open reduction and locking plate internal fixation remain the most popular treatment options (1). The reduction in bone density makes the surgical treatment of proximal humerus fractures more complicated and difficult. Loss of fixation is the most common postoperative complication (occurring in up to 12.8–22.5% of cases) and is among the serious complications that require revision surgery (2-4). Previous studies point to low bone quality as being one of the independent risk factors for reduction loss after surgery for proximal humerus fracture (5,6). Therefore, bone quality is a predictor of surgical reduction quality, and whether sufficient stability can be obtained is critical to ensuring the success of surgery (6).

Several methods for assessing the local bone quality of the proximal humerus have been developed but remain limited. The Tingart index (7) and the deltoid tuberosity index (8) assess cortical bone thickness measurements on anteroposterior views of the shoulder using a 2-dimensional technique. These two methods of measuring cortical bone thickness have been widely investigated in proximal humerus fracture (8,9); however, it has not been determined whether the trabecular thickness (Tb.th) of the humeral trabecular bones change in the process of aging (10). Dual-energy X-ray absorptiometry (DXA) method remains the gold standard for the diagnosis of osteoporosis, but there is not yet a defined threshold value for the proximal humerus (6). Furthermore, those weight-bearing skeletal sides, such as the hip or lumber spine, may misrepresent the true bone mineral density (BMD) of those non-weight-bearing skeletal sides, such as the humerus or radius (11,12). Peripheral quantitative computed tomography (QCT) can qualitatively and quantitatively measure the volume bone density of bone trabeculae with high precision and a relatively low radiation dose (13), but conventional QCT measurements require the use of calibration phantoms, and phantomless QCT for diagnosis of osteoporosis remains a modality reserved for future clinical practice (14-16). None of the abovementioned methods can perform the quantitative analysis of BMD in different areas of the proximal humerus. Therefore, there is an urgent need for a noninvasive, highly reproducible, and multidimensional evaluation of humeral BMD.

Dual-energy computed tomography (DECT) has emerged into clinical routine as an imaging technique with unique postprocessing utilities, with the virtual noncalcium (VNCa) reconstruction algorithm being particularly noteworthy, as it has been used for the quantitative analysis of specific substances, such as iron, calcium, and fat (17-20). VNCa is playing an increasingly important role in BMD quantification, particularly in methods involving phantom and cadaver experiments (21-24). A previous study by Liu *et al.* reported a strong correlation between computed tomography (CT) value of calcium and calcium density derived from DECT (r=0.885, 0.877, respectively, P<0.05) and QCT-based BMD values (24). In their study, the "liver virtual noncontrast (VNC) configuration file" was altered with a specially modified configuration file to produce VNCa values; thus, the output variables were remapped according to calcium rather than iodine values. It has been proven that dual-energy parameters obtained by this method can effectively reflect the BMD of the vertebrae (24).

In addition, bones with a reliable area of biomechanical dominance will help prevent fixation failure. Some studies based on cadaver and finite element models emphasize the importance of screw placement at the posteromedial portion of the proximal humerus (25,26), but this has not been confirmed by local quantitative imaging *in vivo*. Therefore, the purpose of this study was to evaluate the differences in bone quality among 4 regions of the proximal humerus quantitatively using VNCa technology for DECT and to determine the influencing factors [age, sex, body mass index (BMI), region, and VNCa values] on the computed tomography value of calcium (CaCT) derived from DECT.

Methods

Study design and selection of participants

The study was conducted in accordance with the Declaration of Helsinki (as revised in 2013) and was approved by the Ethics Review Committee of Shanghai General Hospital. Individual consent for this retrospective analysis was waived. Data from participants who underwent DECT of the shoulder joint between March 2021 and March 2022 were collected. The participants' demographic characteristics (age, sex, BMI) were recorded. The exclusion criteria were patients with proximal humerus fractures, a history of shoulder surgery (implants, hardware, or other foreign material), severe degenerative changes, and deformity. Finally, 65 participants were included (*Figure 1*).

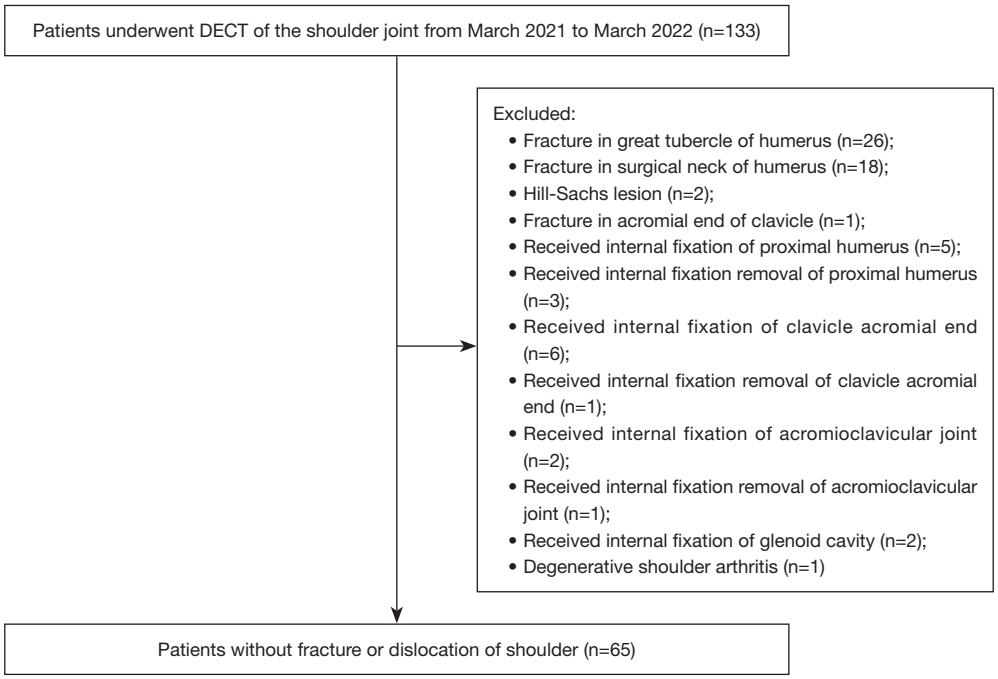

Figure 1 Flowchart of patient selection. DECT, dual-energy computed tomography.

DECT scan protocols and postprocessing

In our study, all shoulder joint examinations of the enrolled participants were performed with a dual-source CT scanner (SOMATOM Definition Force, Siemens Healthineers, Erlangen, Germany) in the supine position and with the shoulder joints in the neutral position, and the scan range was from the acromion to the middle of humeral diaphysis (tube A: 90 kVp, 220 mAs; tube B: 150 kVp with a tin filter, 137 mAs). The scanning parameters were as follows: rotation time, 0.5 seconds; collimation width 128×0.6 mm; and pitch, 0.6.

The default parameters in the liver VNC configuration file were modified according to the bone marrow configuration file of dual-energy analytic software (Syngo.via VB10; Siemens Healthineers). To achieve the quantification of calcium and fat, the default values of soft tissue were revised from 58, 56–52, and 51 Hounsfield units (HU) at 90 and 150 kVp, and those for fat and yellow marrow were the same as the default values (–108 and –84 HU at 90 and 150 kVp, respectively). The iodine slope of 3.01 was replaced with the calcium slope of 1.71 (18,24,27). Thus, the quantitative parameters of the liver VNC and the CT value for the contrast media and the contrast agent density were replaced by the CT value for calcium and calcium density, respectively.

Through adjustment of the multiplanar reformation images to achieve a standard transversal plane, the 2 ends of the articular surface of the humerus head were connected to make a vertical bisector; thus, the humerus head was divided into 4 regions. The round region of interest (ROI) was delineated in as large as possible area in the medial plane between the greater tuberosity and the surgical neck, with the cortical bone being avoided (*Figure 2*) (28).

The VNCa value, CaCT, computed tomography value of mixed-energy images (regular CT value) (rCT), and relative calcium density (rCaD) were measured for each humerus. All measurements were performed independently at the postprocessing workstation by a radiologist with 4 years of experience in the diagnosis of musculoskeletal disease.

Statistical analysis

All statistical analyses were powered by standard software (SPSS v. 20.0, IBM Corp., Armonk, NY, USA). Continuous variables are expressed as the mean ± standard deviations (SDs) or as medians with interquartile range as appropriate, and categorical variables are reported as proportions. The normality of continuous variables was assessed using the Kolmogorov-Smirnov test. Depending on whether

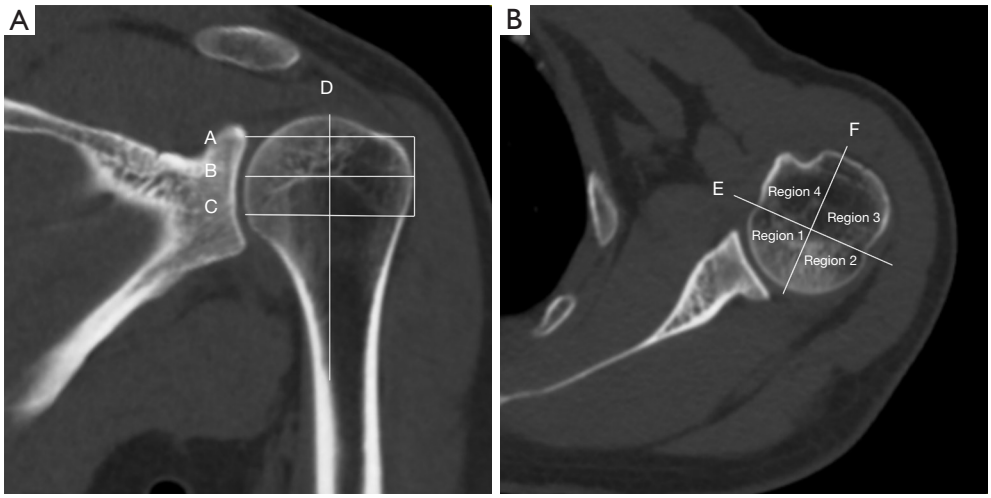

Figure 2 Defining 4 regions of humeral head. (A) Coronal plane: line D is parallel to the long axis of the humeral shaft, line A and C are perpendicular to the line D. Line B is the medial plane between the greater tuberosity (line A) and the surgical neck (line C). (B) Corresponding transverse plane on line B: the process for dividing the humeral head into 4 regions is as follows: line E connects the 2 ends of the articular surface of the humeral head, and line F bisects line E vertically. Regions 1–4 are the anteromedial, posteromedial, posterolateral, and anterolateral regions of the humeral head, respectively.

the quantitative parameters (VNCa, CaCT, rCT, rCaD) conformed to normal distribution, differences between males and females were tested using the independent samples *t*-test or the Mann-Whitney test. One-way analysis of variance (ANOVA) or Friedman were implemented for the analysis among the 4 regions of the proximal humeri. According to whether these quantitative parameters (VNCa, CaCT, rCT, rCaD) conformed to a homogeneity test of variance, the Tukey test or Games-Howell test was used for between-group comparisons. Levene test was used to test the homogeneity of variance of variables. Spearman correlation analysis was applied to determine correlations between age, BMI, and individual quantitative parameters. Multivariable linear regression analysis was used to determine the influence of CaCT, age, sex, and BMI on the VNCa value. P<0.05 was considered statistically significant.

Results

A total of 65 patients were evaluated, aged from 21 to 80 years (average 49.5±15.2 years). Participant demographics and characteristics are outlined in *Table 1*.

Differences in the VNCa value, CaCT, rCT, and rCaD among the 4 regions of the proximal humeri

There were no significant differences in the VNCa value among the 4 regions of the humeral head (P=0.688) among the 4 regions of the proximal humeri. As there were no statistical differences in the overall comparison, a comparison between groups was not conducted. There were statistically significant differences in individual quantitative parameters (CaCT, rCT, rCaD) among the 4 regions of the proximal humeri (all P values <0.001), and there were also statistical differences between all group comparisons (all P values <0.05) (*Figure 3*). Among them, the CaCT, rCT, and rCaD of region 2 were the highest, followed by those of region 1, region 3, and region 4. It is worth mentioning that there were no statistically significant differences in rCT between the anteromedial and posteromedial regions of the proximal humeri (P>0.05), while there were statistically significant differences in CaCT and rCaD (P<0.05) (*Table 2*, *Figure 3*).

Differences between males and females

There were no statistically significant differences in the VNCa value of the proximal humeri between males and females. There were statistically significant differences in the quantitative parameters (CaCT, rCT, rCaD) of the 4 regions between males and females (P<0.05) but not for the posterolateral zone (rCT; P>0.05) (*Table 3*, *Figure 4*).

Table 1 Participant demographics

Item	Male	Female
Number, n [%]	32 [49]	33 [51]
Age (years)		
Mean ± SD	47.6±15.1	51.3±15.3
95% CI	42.2–53.1	45.9–56.7
BMI (kg/m^2)		
Mean ± SD	23.4±3.1	24.0±3.8
95% CI	22.3–24.5	22.7–25.3

SD, standard deviation; CI, confidence interval; BMI, body mass index.

Correlation of age, sex, BMI, region, and VNCa values on CaCT

Spearman correlation analysis showed that age and BMI had no correlation with VNCa value (P>0.05), and BMI had no correlation with DECT parameters (VNCa, CaCT, rCT, rCaD; P>0.05) among the 4 regions of the proximal humeri. The results also showed that age was negatively correlated with quantitative parameters (CaCT, rCT, rCaD) among the 4 regions of the proximal humeri (P<0.05) (*Table 4*).

Multivariable linear regression analysis showed that the correlation of age, sex, BMI, region of the proximal humerus, and VNCa values with CaCT was significant (F=95.454; R^2=0.653; P<0.001). The predicted CaCT value was calculated as follows: CaCT =344.755–35.167 sex

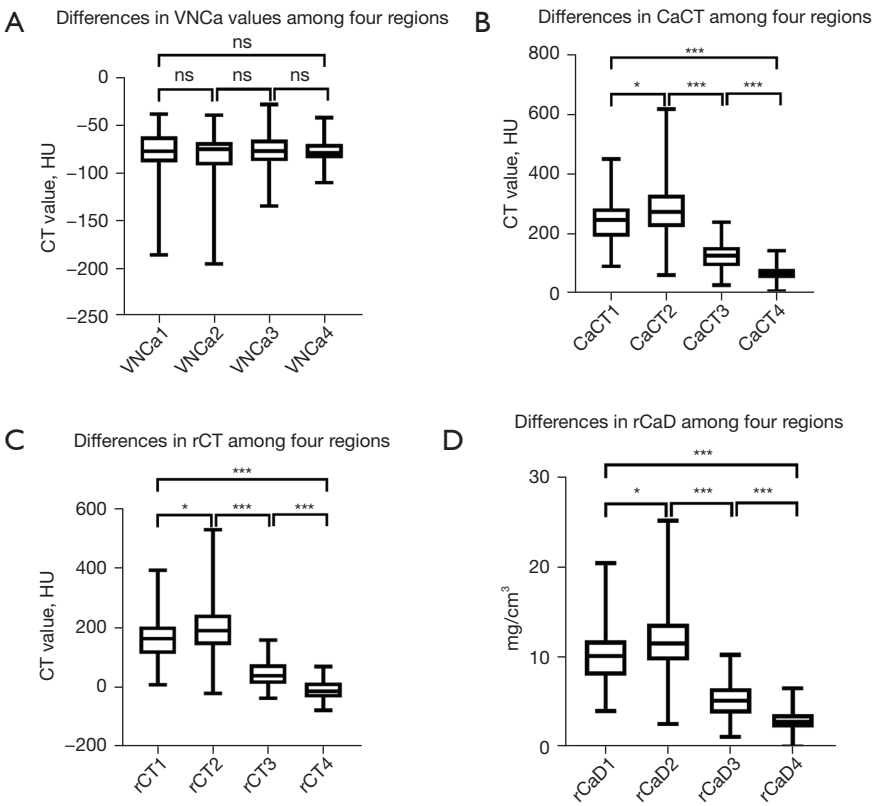

Figure 3 Differences in the VNCa values (A), CaCT (B), rCT (C), and rCaD (D) among the 4 regions of the proximal humeri. ns, no significance; *, P≤0.05; ***, P<0.001. VNCa, virtual noncalcium; CaCT, computed tomography value of calcium; rCT, computed tomography value of mixed-energy images (regular CT value); rCaD, relative calcium density; CT, computed tomography.

Table 2 Descriptive statistics of the humeral head (n=65)

Region	VNCa (HU)	CaCT (HU)	rCT (HU)	rCaD (mg/cm^3)
1	−78.6±22.7	238.8±70.6	160.7±66.3	10.0±3.0
2	−75.4 (−92.4 to 68.0)[a]	281.7±90.0	201.0±84.9	11.9±3.8
3	−77.4 (−87.8 to 65.6)[a]	124.5±45.7	48.3±45.6	5.3±1.9
4	−77.5±12.3	68.7±32.8	−8.9±31.9	3.0±1.4
P	0.688*	<0.001**	<0.001**	<0.001**
P$^{1-2}$***		0.016	0.016	0.014
P$^{1-3}$***		<0.001	<0.001	<0.001
P$^{1-4}$***		<0.001	<0.001	<0.001
P$^{2-3}$***		<0.001	<0.001	<0.001
P$^{2-4}$***		<0.001	<0.001	<0.001
P$^{3-4}$***		<0.001	<0.001	<0.001

Unless specifically mentioned, all data are mean ± standard deviation. [a], values are medians with interquartile ranges in parentheses. *, Friedman test was used to compare differences among the 4 parts; as there were no statistical differences during overall comparison, the comparison between groups was not conducted; **, one-way analysis of variance was used to compare differences among the 4 parts; ***, Games-Howell test was used to compare differences between groups. P<0.05 indicates a significant difference. Regions 1–4 are the anteromedial, posteromedial, posterolateral, and anterolateral regions of the humeral head, respectively. VNCa, virtual noncalcium; CaCT, computed tomography value of calcium; rCT, computed tomography value of mixed-energy images (regular CT value); rCaD, relative calcium density; CT, computed tomography.

Table 3 Comparison of VNCa value, CaCT, rCT, and rCaD between males and females

Region	Sex/P	VNCa (HU)	CaCT (HU)	rCT (HU)	rCaD (mg/cm^3)
1	M[a]	−79.7 (−91.8 to 63.0)	281.5 (237.1 to 304.8)	186.6 (160.8 to 226.6)	11.6 (10.0 to 12.9)
	F[b]	−75.5±18.7	205.0±60.3	129.9±60.4	8.6±2.5
	P*	0.352	<0.001	<0.001	<0.001
2	M[a]	−79.2 (−94.7 to 69.4)	295.4 (247.0 to 338.7)	219.4 (170.2 to 263.8)	12.6 (10.7 to 14.5)
	F[b]	−77.3±20.6	249.7±66.5	172.8±66.7	10.5±2.9
	P*	0.306	0.005	0.006	0.005
3	M[b]	−79.5±17.5	138.3±42.6	59.3±42.6	5.9±1.8
	F[b]	−73.8±17.3	111.2±45.3	37.6±46.5	4.7±1.9
	P**	0.191	0.016	0.055	0.013
4	M[b]	−77.5±11.1	80.7±30.4	3.0±30.3	3.4±1.3
	F[b]	−77.5±13.5	57.1±31.3	−20.4±29.4	2.6±1.3
	P**	0.994	0.003	0.002	0.023

[a], values are medians with interquartile ranges in parentheses; [b], values are mean ± standard deviation. *, independent samples *t*-test was used to compare differences between groups; **, Mann-Whitney test was used to compare differences between groups. P<0.05 indicates a significant difference. Regions 1–4 are the anteromedial, posteromedial, posterolateral, and anterolateral regions of the humeral head, respectively. VNCa, virtual noncalcium; CaCT, computed tomography value of calcium; rCT, computed tomography value of mixed-energy images (regular CT value); rCaD, relative calcium density; CT, computed tomography; M, male; F, female.

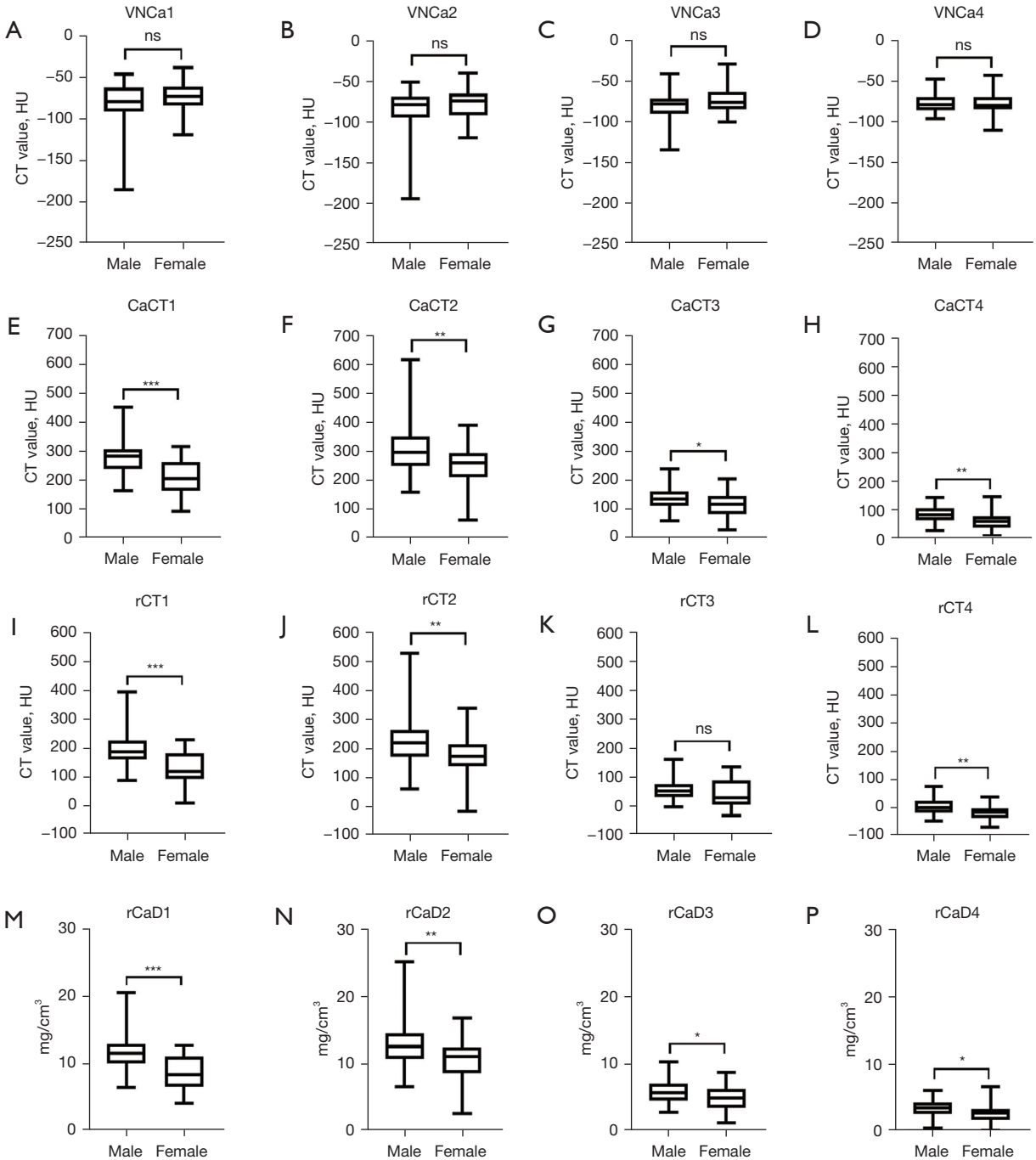

Figure 4 Differences in VNCa values (A-D), CaCT (E-H), rCT (I-L), and rCaD (M-P) for the 4 regions of proximal humerus between males and females. ns, no significance; *, P≤0.05; **, P≤0.01; ***, P≤0.001. VNCa, virtual noncalcium; CaCT, computed tomography value of calcium; rCT, computed tomography value of mixed-energy images (regular CT value); rCaD, relative calcium density; CT, computed tomography.

Table 4 Correlation of age and BMI with VNCa, CaCT, rCT, and rCaD

Region	Item	r/P	VNCa	CaCT	rCT	rCaD
1	Age	r	–0.119	–0.549	–0.602	–0.537
		P	0.347	<0.001	<0.001	<0.001
	BMI	r	0.028	0.148	0.154	0.163
		P	0.827	0.239	0.220	0.193
2	Age	r	–0.084	–0.663	–0.714	–0.594
		P	0.503	<0.001	<0.001	<0.001
	BMI	r	–0.201	0.199	0.135	0.243
		P	0.108	0.112	0.283	0.051
3	Age	r	0.054	–0.399	–0.351	–0.377
		P	0.668	0.001	0.004	0.002
	BMI	r	0.193	0.105	0.159	0.105
		P	0.124	0.407	0.207	0.405
4	Age	r	–0.110	–0.436	–0.492	–0.384
		P	0.382	<0.001	<0.001	0.002
	BMI	r	0.097	0.056	0.101	0.022
		P	0.440	0.658	0.421	0.862

Regions 1–4 are the anteromedial, posteromedial, posterolateral, and anterolateral regions of the humeral head, respectively. P<0.05 indicates a significant difference. VNCa, virtual noncalcium; CaCT, computed tomography value of calcium; rCT, computed tomography value of mixed-energy images (regular CT value); rCaD, relative calcium density; CT, computed tomography; BMI, body mass index.

–1.945 age –65.908 regions –1.101 VNCa +2.589 BMI. In this model, sex, age, BMI, region, and VNCa were significant (P<0.05) predictors of the CaCT value.

Discussion

In our study, we used a liver VNC algorithm of DECT to quantitatively evaluate the bone marrow composition and distribution of cancellous bone in the proximal humerus. By altering the liver VNC file with a specially modified configuration file, we produced a VNCa file, in which the CT value for contrast media and the contrast agent density correspond to the CaCT and the calcium density, respectively. A previous study showed that VNCa technology can be used as a reference standard for detecting lumbar osteoporosis, with a sensitivity of 90% and a specificity of 92% (24). Our study demonstrated that the calcium concentration (CaCT, rCaD) was the highest in the posteromedial zone of the humeral head and the lowest in the greater tuberosity, which is the site of osteoporotic fracture. Except for the VNCa value, these quantitative parameters (CaCT, rCT, rCaD) were significantly different among the 4 regions of the humeral head and between males and females. We also investigated whether age, sex, regions, BMI, and VNCa value correlated with CaCT. The results showed that sex, age, BMI, region of the proximal humerus, and VNCa value were correlated to a degree with CaCT.

In this study, the VNCa technology of DECT was used to evaluate the bone marrow composition in different regions of the proximal humerus. This is different from the approach used in other studies (7,8,10,29,30). A previous study by Zhang *et al.* measured the proximal humerus computed tomography values (CT_{Mean}) in patients with fracture (29). They found that the proximal humerus CT_{Mean} measured with a single-source spiral CT was closely related to the BMD in the lumbar spine and femoral neck measured with DXA. However, the pixel value or CT number entirely depends on the linear attenuation coefficient (μ), which has considerable overlap between different body materials. In thick body regions, such as the shoulder, Compton

scattering and beam hardening of hyperdense cortical bone are pronounced and affect the CT value of bone marrow. In this study, VNCa imaging was used to evaluate the bone marrow, which is beyond the scope of single-source spiral CT evaluation.

The humeral head was divided into 4 regions in this study. The results indicated no statistically significant differences in rCT, but statistically significant differences in CaCT and rCaD between the anteromedial and posteromedial regions were found. For conventional CT, the CT values of the bones are mainly determined by the trabecular structure, so rCT can reflect the osteoporosis of bones to a certain extent (14,31). The VNCa image is calculated by subtracting the relative attenuation attributed to calcium from the total attenuation (32), The quantitative parameters of CaCT and rCaD reflect the CT value and concentration of calcium quantitatively (33), which are key components of BMD and better explain the difference in calcium content in the proximal humerus than does rCT. We found that the calcium concentration was the highest in the posteromedial zone of the humeral head and the lowest in the greater tuberosity, which is consistent with previous studies (10,34). Previous biomechanical studies have demonstrated the importance of screw placement on the posteromedial proximal humerus (25,26,35), and Tingart *et al.* (25) showed that placing screws in areas with a higher bone density may help to prevent loosening of the internal fixation and improve patient outcomes. These results indicated that areas with higher bone density can help indicate the optimal areas for operation after proximal humerus fractures to prevent loosening or failing implants.

In a previous study by Zhang *et al.* (29), the incidence of osteoporosis for those with proximal humerus fractures was higher in older adult females than in males of the same age group. The findings of our study are consistent with those of Zhang *et al.* (29). The quantitative parameters (CaCT, rCT, rCaD) of the proximal humerus in males were significantly higher than those in females. It has been shown that the sex difference may be attributed to severe osteoporosis caused by an early and rapid drop in estrogen levels in females (36). The prevalence of osteoporotic fractures of the proximal humerus increases with age, and reports indicate that osteoporosis is significantly higher in women than in men in the European Union (37,38). In addition, accidental injury is a common cause of proximal humerus fractures, with two-thirds of accidental fractures occurring in women (29,38). One study reported gender differences in bone density among osteoporosis, osteopenia, and normal bone mass groups, with the extent of bone mass loss in women being more severe than that in men (29).

In this study, we investigated whether BMI influences CaCT. There were no correlations between CaCT, rCT, rCaD, and BMI in any of the 4 regions, which is in line with previous research (30,31). Unlike lumbar vertebrae, femoral neck, and other weight-bearing bone joints (39), the BMD in the proximal humerus was not significantly associated with BMI. The effect of BMI on BMD would mask the loss of bone, while the non-weight-bearing area, such as the proximal humerus, reduced the effect of BMI on BMD (30).

There were several limitations in this study. First, this study did not compare calcium content obtained with VNCa in the proximal humerus with BMD obtained with DXA. Second, information on prescription medicine was not available, and we did not enroll a specific group of patients, such as those with severe degenerative changes, fractures, or tumors, or those in the postoperative stage etc. Rather, we decided to examine the effects of medicine on BMD in the proximal humerus and the characteristics of BMD of the proximal humerus in other types of patients. Third, the study only included a Chinese population in 1 hospital, and the results should be interpreted with caution when applied to other ethnic groups.

Conclusions

In conclusion, this study investigated the calcium distribution in the humeral head. The results suggest the concentration of calcium to be the densest in the posteromedial region of the humeral head. VNCa technology with DECT may be used for the quantification of proximal humerus BMD.

Acknowledgments

Funding: None.

Footnote

Conflicts of Interest: All authors have completed the ICMJE uniform disclosure form (available at https://qims.amegroups.com/article/view/10.21037/qims-22-927/coif). ZX is an employee of Siemens Healthineers; however, control of all data and information submitted for publication was given to the authors who were not affiliated with Siemens Healthineers. The other authors have no conflicts of interest to declare.

Ethical Statement: The authors are accountable for all aspects of the work in ensuring that questions related to the accuracy or integrity of any part of the work are appropriately investigated and resolved. The study was conducted in accordance with the Declaration of Helsinki (as revised in 2013) and was approved by the Ethics Review Committee of Shanghai General Hospital. Individual consent for this retrospective analysis was waived.

References

1. Tepass A, Blumenstock G, Weise K, Rolauffs B, Bahrs C. Current strategies for the treatment of proximal humeral fractures: an analysis of a survey carried out at 348 hospitals in Germany, Austria, and Switzerland. J Shoulder Elbow Surg 2013;22:e8-14.
2. Carbone S, Papalia M. The amount of impaction and loss of reduction in osteoporotic proximal humeral fractures after surgical fixation. Osteoporos Int 2016;27:627-33.
3. Haasters F, Siebenbürger G, Helfen T, Daferner M, Böcker W, Ockert B. Complications of locked plating for proximal humeral fractures-are we getting any better? J Shoulder Elbow Surg 2016;25:e295-303.
4. Sproul RC, Iyengar JJ, Devcic Z, Feeley BT. A systematic review of locking plate fixation of proximal humerus fractures. Injury 2011;42:408-13.
5. Jung SW, Shim SB, Kim HM, Lee JH, Lim HS. Factors that Influence Reduction Loss in Proximal Humerus Fracture Surgery. J Orthop Trauma 2015;29:276-82.
6. Spross C, Zeledon R, Zdravkovic V, Jost B. How bone quality may influence intraoperative and early postoperative problems after angular stable open reduction-internal fixation of proximal humeral fractures. J Shoulder Elbow Surg 2017;26:1566-72.
7. Tingart MJ, Apreleva M, von Stechow D, Zurakowski D, Warner JJ. The cortical thickness of the proximal humeral diaphysis predicts bone mineral density of the proximal humerus. J Bone Joint Surg Br 2003;85:611-7.
8. Spross C, Kaestle N, Benninger E, Fornaro J, Erhardt J, Zdravkovic V, Jost B. Deltoid Tuberosity Index: A Simple Radiographic Tool to Assess Local Bone Quality in Proximal Humerus Fractures. Clin Orthop Relat Res 2015;473:3038-45.
9. Kim DM, Park D, Kim H, Lee ES, Shin MJ, Jeon IH, Koh KH. Risk Factors for Severe Proximal Humerus Fracture and Correlation Between Deltoid Tuberosity Index and Bone Mineral Density. Geriatr Orthop Surg Rehabil 2020;11:2151459320938571.
10. Barvencik F, Gebauer M, Beil FT, Vettorazzi E, Mumme M, Rupprecht M, Pogoda P, Wegscheider K, Rueger JM, Pueschel K, Amling M. Age- and sex-related changes of humeral head microarchitecture: histomorphometric analysis of 60 human specimens. J Orthop Res 2010;28:18-26.
11. Handa A, Uchiyama Y, Shinpuku E, Watanabe M. Comparison of three plain radiography methods for evaluating proximal humerus bone strength in women. J Orthop Sci 2019;24:243-9.
12. Wilson J, Bonner TJ, Head M, Fordham J, Brealey S, Rangan A. Variation in bone mineral density by anatomical site in patients with proximal humeral fractures. J Bone Joint Surg Br 2009;91:772-5.
13. Ma J, Zhao J, He W, Kuang M, Chen H, Zhang L, Sun L, Cui Y, Ma X, Wang Y. Review of high-resolution peripheral quantitative computed tomography for the assessment of bone microstructure and strength. Sheng Wu Yi Xue Gong Cheng Xue Za Zhi 2018;35:468-74.
14. Gruenewald LD, Koch V, Martin SS, Yel I, Eichler K, Gruber-Rouh T, Lenga L, Wichmann JL, Alizadeh LS, Albrecht MH, Mader C, Huizinga NA, D'Angelo T, Mazziotti S, Wesarg S, Vogl TJ, Booz C. Diagnostic accuracy of quantitative dual-energy CT-based volumetric bone mineral density assessment for the prediction of osteoporosis-associated fractures. Eur Radiol 2022;32:3076-84.
15. Xiongfeng T, Cheng Z, Meng H, Chi M, Deming G, Huan Q, Bo C, Kedi Y, Xianyue S, Tak-Man W, William Weijia L, Yanguo Q. One Novel Phantom-Less Quantitative Computed Tomography System for Auto-Diagnosis of Osteoporosis Utilizes Low-Dose Chest Computed Tomography Obtained for COVID-19 Screening. Front Bioeng Biotechnol 2022;10:856753.
16. Zhou S, Zhu L, You T, Li P, Shen H, He Y, Gao H, Yan L, He Z, Guo Y, Zhang Y, Zhang K. In vivo quantification of bone mineral density of lumbar vertebrae using fast kVp switching dual-energy CT: correlation with quantitative

computed tomography. Quant Imaging Med Surg 2021;11:341-50.
17. Fischer MA, Reiner CS, Raptis D, Donati O, Goetti R, Clavien PA, Alkadhi H. Quantification of liver iron content with CT-added value of dual-energy. Eur Radiol 2011;21:1727-32.
18. Luo XF, Xie XQ, Cheng S, Yang Y, Yan J, Zhang H, Chai WM, Schmidt B, Yan FH. Dual-Energy CT for Patients Suspected of Having Liver Iron Overload: Can Virtual Iron Content Imaging Accurately Quantify Liver Iron Content? Radiology 2015;277:95-103.
19. Molwitz I, Leiderer M, McDonough R, Fischer R, Ozga AK, Ozden C, Tahir E, Koehler D, Adam G, Yamamura J. Skeletal muscle fat quantification by dual-energy computed tomography in comparison with 3T MR imaging. Eur Radiol 2021;31:7529-39.
20. Peng Y, Ye J, Liu C, Jia H, Sun J, Ling J, Prince M, Li C, Luo X. Simultaneous hepatic iron and fat quantification with dual-energy CT in a rabbit model of coexisting iron and fat. Quant Imaging Med Surg 2021;11:2001-12.
21. Qin L, Huang J, Yu P, Yan J, Ge Y, Lu Y, Yan F, Wang L, Du L. Accuracy, agreement, and reliability of DECT-derived vBMD measurements: an initial ex vivo study. Eur Radiol 2021;31:191-9.
22. Koch V, Hokamp NG, Albrecht MH, Gruenewald LD, Yel I, Borggrefe J, et al. Accuracy and precision of volumetric bone mineral density assessment using dual-source dual-energy versus quantitative CT: a phantom study. Eur Radiol Exp 2021;5:43.
23. Roski F, Hammel J, Mei K, Baum T, Kirschke JS, Laugerette A, Kopp FK, Bodden J, Pfeiffer D, Pfeiffer F, Rummeny EJ, Noël PB, Gersing AS, Schwaiger BJ. Bone mineral density measurements derived from dual-layer spectral CT enable opportunistic screening for osteoporosis. Eur Radiol 2019;29:6355-63.
24. Liu Z, Zhang Y, Liu Z, Kong J, Huang D, Zhang X, Jiang Y. Dual-Energy Computed Tomography Virtual Noncalcium Technique in Diagnosing Osteoporosis: Correlation With Quantitative Computed Tomography. J Comput Assist Tomogr 2021;45:452-7.
25. Tingart MJ, Lehtinen J, Zurakowski D, Warner JJ, Apreleva M. Proximal humeral fractures: regional differences in bone mineral density of the humeral head affect the fixation strength of cancellous screws. J Shoulder Elbow Surg 2006;15:620-4.
26. Li B, Chang S, Hu S, Du S, Xiong W. Three-dimensional finite element analysis of exo-cortical placement of humeral calcar screw for reconstruction of medial column stability. Zhongguo Xiu Fu Chong Jian Wai Ke Za Zhi 2022;36:995-1002.
27. Wang Lin, Chen C, Gong S, Gu K, He B, Yan S, Ruan X, He S. Dual-energy CT virtual non-contrast Technology in the diagnosis of osteoporosis: a preliminary study. Chinese Journal of Radiology 2017;51:949-53.
28. Cheng L, Wu X, Chai Y. Clinical assessment of cancellous bone content in the humeral head. Chinese Journal of Trauma 2011;13:4.
29. Zhang X, Zhu CX, He JQ, Hu YC, Sun J. Correlation of CT Values and Bone Mineral Density in Elderly Chinese Patients with Proximal Humeral Fractures. Orthop Surg 2021;13:2271-9.
30. Zhu Q, Fu Z, Zhang D, Jiang B. Measurement of bone mineral density in the proximal humeral region. Chinese Journal of Trauma 2009;(12):523-6.
31. Pervaiz K, Cabezas A, Downes K, Santoni BG, Frankle MA. Osteoporosis and shoulder osteoarthritis: incidence, risk factors, and surgical implications. J Shoulder Elbow Surg 2013;22:e1-8.
32. Petritsch B, Kosmala A, Weng AM, Krauss B, Heidemeier A, Wagner R, Heintel TM, Gassenmaier T, Bley TA. Vertebral Compression Fractures: Third-Generation Dual-Energy CT for Detection of Bone Marrow Edema at Visual and Quantitative Analyses. Radiology 2017;284:161-8.
33. Müller FC, Gosvig KK, Mikkel Ø, Bjarne R, Rodell A, Henrik B, Krauss B, Gade JS, Boesen M. Quantifying the bone marrow composition of the healthy adult wrist with dual-energy CT. Eur J Radiol 2021;139:109725.
34. Tingart MJ, Bouxsein ML, Zurakowski D, Warner JP, Apreleva M. Three-dimensional distribution of bone density in the proximal humerus. Calcif Tissue Int 2003;73:531-6.
35. Omid R, Trasolini NA, Stone MA, Namdari S. Principles of Locking Plate Fixation of Proximal Humerus Fractures. J Am Acad Orthop Surg 2021;29:e523-35.
36. Lo JC, Chandra M, Lee C, Darbinian JA, Ramaswamy M, Ettinger B. Bone Mineral Density in Older U.S. Filipino, Chinese, Japanese, and White Women. J Am Geriatr Soc 2020;68:2656-61.
37. Roux A, Decroocq L, El Batti S, Bonnevialle N, Moineau G, Trojani C, Boileau P, de Peretti F. Epidemiology of proximal humerus fractures managed in a trauma center. Orthop Traumatol Surg Res 2012;98:715-9.
38. Hernlund E, Svedbom A, Ivergård M, Compston J, Cooper C, Stenmark J, McCloskey EV, Jönsson B, Kanis JA. Osteoporosis in the European Union: medical

management, epidemiology and economic burden. A report prepared in collaboration with the International Osteoporosis Foundation (IOF) and the European Federation of Pharmaceutical Industry Associations (EFPIA). Arch Osteoporos 2013;8:136.

39. Wen Y, Li H, Zhang X, Liu P, Ma J, Zhang L, Zhang K, Song L. Correlation of Osteoporosis in Patients With Newly Diagnosed Type 2 Diabetes: A Retrospective Study in Chinese Population. Front Endocrinol (Lausanne) 2021;12:531904.

Cite this article as: Yu Q, Yang J, Zhou C, Xu Z, Liu C, Luo Q, Zhang L. Quantification of bone quality and distribution of the proximal humerus with dual-energy computed tomography. Quant Imaging Med Surg 2023;13(9):5676-5687. doi: 10.21037/qims-22-927

